

# Correcting Incompatible DN Values and Geometric Errors in Nighttime Lights Time-Series Images

Naizhuo Zhao, Yuyu Zhou, and Eric L. Samson

**Abstract**—The Defense Meteorological Satellite Program’s Operational Linescan System (DMSP-OLS) nighttime lights imagery has proven to be a powerful remote sensing tool to monitor urbanization and assess socioeconomic activities at large scales. However, the existence of incompatible digital number (DN) values and geometric errors severely limit application of nighttime light image data on multiyear quantitative research. In this paper, we extend and improve previous studies on intercalibrating nighttime lights image data to obtain more compatible and reliable nighttime lights time-series (NLT) image data for China and the U.S. through four steps, namely, intercalibration, geometric correction, steady-increase adjustment, and population data correction. We then use gross domestic product (GDP) data to test the processed NLT image data indirectly and find that sum light (summed DN value of pixels in a nighttime light image) maintains apparent increase trends with relatively large GDP growth rates but does not increase or decrease with relatively small GDP growth rates. As nighttime light is a sensitive indicator for economic activity, the temporally consistent trends between sum light and GDP growth rate imply that brightness of nighttime lights on the ground is correctly represented by the processed NLT image data. Finally, through analyzing the corrected NLT image data from 1992 to 2008, we find that China experienced apparent nighttime lights development in 1992–1997 and 2001–2008, respectively, and the U.S. showed nighttime lights decay in large areas after 2001.

**Index Terms**—Geometric error, gross domestic product (GDP), nighttime lights development/decay, nighttime lights time-series (NLT) images.

## I. INTRODUCTION

THE Defense Meteorological Satellite Program’s Operational Linescan System (DMSP-OLS) nighttime lights time-series (NLT) image products are a unique remote sensing data set to observe global socioeconomic activities at a relatively high spatial resolution (1 km × 1 km) and across a relatively long period relative to remote sensing data sets (1992–2012) [1]. However, two critical temporal drawbacks of the NLT image products greatly limit application of the image products for quantitative multiyear research: NLT image

products are not radiometrically calibrated; thus, digital number (DN) values are incompatible across different years [2], and geometric errors exist in the NLT image products that lead to spatial inconsistency over different years [3], [4].

To solve the problem of incompatible DN values, Elvidge *et al.* [2] developed a method in which empirically developed second-order regression functions were used to intercalibrate NLT image products because no on-board calibration system existed. The key to the approach of Elvidge *et al.* is to assume Sicily, Italy to be a region with no change in nighttime lights from 1994 to 2008. The 1999 annual image composite collected by DMSP satellite F12 is selected as a reference image because data from this annual image composite have the largest DN values [2]. A group of second-order regression functions was developed by adjusting DN values of pixels in Sicily of candidate images to the match DN values of pixels in Sicily in the reference image. The second-order functions are then used to calibrate their corresponding nighttime light images. Although comparability of the NLT image products can be greatly enhanced by the second-order-function intercalibration, the method is not without error as it is highly improbable that nighttime lights in Sicily did not experience any changes from 1992 to 2012 (i.e., a temporal extent of currently available NLT image products). After the intercalibration, DN values in NLT image products are still not completely compatible, which can be reflected by remaining discrepancies in sum light (summed DN value of pixels in a nighttime light image) or lit area (areal extent of nighttime lights) between two satellites for the same year [5], [6].

To further improve comparability and continuity of NLT image products, Liu *et al.* [5] adjusted the intercalibrated NLT images based on another supposition in which each pixel’s DN value in an early NLT image should not be larger than that in a later NLT image. The adjusted NLT images were then used to map urban expansion in China [5]. The assumption of Liu *et al.* [5] seems workable for China, a rapidly developing country in economy and urbanization. However, relatively large errors will be produced when the method of Liu *et al.* [5] is applied to developed countries where urban decline has widely emerged in the 20th century [7]. Economic crises, deindustrialization, rising city crime rates, etc., have resulted in population decline in many post-industrial cities, particularly in the U.S. [7]–[10]. Such urban depopulation is very likely to lead to decrease in brightness of nighttime lights in particular districts of cities (e.g., industrial areas), making it necessary to develop a more reliable and universal method to calibrate and correct DN values in NLT images than the assumptions of Liu *et al.* [5].

Manuscript received April 1, 2014; revised June 30, 2014; accepted August 21, 2014. This work was supported by the NASA ROSES Land-Cover/Land-Use Change Program under Grant NNH11ZDA001N-LCLUC. (Corresponding author: Yuyu Zhou.)

N. Zhao is with the Department of Geoscience, Texas Tech University, Lubbock, TX 79409 USA.

Y. Zhou is with the Joint Global Change Research Institute, Pacific Northwest National Laboratory, College Park, MD 20749 USA (e-mail: yuyu.zhou@pnnl.gov).

E. L. Samson is with the Mayan Esteem Project, Farmington, CT 06032 USA.

Color versions of one or more of the figures in this paper are available online at <http://ieeexplore.ieee.org>.

Digital Object Identifier 10.1109/TGRS.2014.2352598

In contrast to much attention around intercalibrating incompatible DN values in NLT images, very limited effort has been given to correct geometric errors in NLT images. Geometric errors were generated when many scenes of nighttime light imagery were mosaicked to create an annual image product [3]. When NLT images were used to map urban expansion, the geometric errors reduced spatial consistency and consequently resulted in incompatible urban extents across different years. Liu *et al.* [5] found that some pixels were lit in one annual image product but unlit in another for the same year. They treated these as unstable lit pixels and revalued the pixels as 0. However, if the pixels are located at peripheries of individual lit regions, geometric errors might be occurring explaining such pixels being lit in one annual image but unlit in another for the same year. Thus, further correction on DN values of the NLT images should be conducted after any elaborate geometric correction is finished.

As the largest developing and developed countries, respectively, China's and the U.S.' economic growth and urban development have greatly impacted global social and ecological systems [11]. Many scholars have used NLT images to map urban expansion and assess economic development in these two countries [5], [11]–[20]. However, the problem of geometric errors was neglected in all previous studies, and the incompatible DN values were not corrected to the best extent. Therefore, the main objectives of this paper are to correct incompatible DN values and geometric errors in NLT images for China and the U.S. To fulfill these study objectives, we extend and improve previous methods proposed by Elvidge *et al.* [2] and Liu *et al.* [5] to preliminarily calibrate and use gridded population data to further adjust DN values in NLT images. Additionally, we correct geometric errors in NLT images based on a shift-based method. Finally, we evaluate the dependability of the processed NLT image data reflecting actual changes in ground nighttime lights through comparison with statistical gross domestic product (GDP) growth rates.

## II. DATA

The version 4 DMSP-OLS NLT image products were obtained from the National Oceanic and Atmospheric Administration's National Geophysical Data Center (NGDC) (available from: <http://ngdc.noaa.gov/eog/dmsp/downloadV4composites.html>; last access June 9, 2014). The NLT image products were produced by all available cloud-free nighttime light images for any given calendar year in the NGDC's digital archive and have a 30-arcsec ( $\sim 1$  km) spatial resolution. The NLT image products have two types of subproducts: 1) average DN value image composites; and 2) average DN value multiplied by the percent frequency of light detection image composites. Compared to average DN value image composites, DN values in an average DN value multiplied by the percent frequency of light detection image composite more accurately represent brightness of nighttime lights for the whole year due to consideration of the frequency of light detection. Thus, in this paper, we used average DN value multiplied by the percent frequency of light detection image composites (hereafter, still referred to as NLT

image products). Additionally, 2008 is the last year of gridded population data that we can obtain. Consequently, in this paper, we intercalibrated and corrected NLT image data from 1992 to 2008 although current NLT image products cover 21 years (i.e., from 1992 to 2012). Detailed algorithms and processes for the annual image composites have been described by Elvidge *et al.* [2] and Baugh *et al.* [21].

Global Rural-Urban Mapping Project's (GRUMP's) population density grid data of 1990, 1995, and 2000 were collected from the NASA's Socioeconomic Data and Applications Center (SEDAC) for improving compatibility and continuity of NLT image products [22]. The GRUMP's gridded population data have the same spatial resolution [30 arcsec ( $\sim 1$  km)] as NLT image products and were produced by a census-data-centered approach, in which population density was obtained directly from national government censuses and settlement areas were determined by the GIS data of Balk *et al.* [23]. After 2000, the GRUMP's population density data set with a 30-arcsec spatial resolution was no longer updated; hence, we selected LandScan population data for 2008 obtained from the Oak Ridge National Laboratory for improving compatibility and continuity of NLT images later than 2000 [24]. The LandScan population data set was produced by a remotely sensed-data-centered approach, in which the best available census data (mostly at province/state level) are distributed to each  $1 \text{ km} \times 1 \text{ km}$  pixel mainly by remotely sensed data [25]. Accuracy of the LandScan population data set for the Southwest U.S. has been evaluated with the overall correspondence with census data at 87.8% [25].

Nighttime light imagery has been used in producing the GRUMP and the LandScan gridded population data. However, the problem of recursive referencing of nighttime lights will not emerge when the GRUMP and the LandScan population data are used to improve compatibility and continuity of NLT image products in this paper because, in the GRUMP, nighttime light imagery is just used to delimit areal extents of human settlements and typically cannot influence population counts of individual cells [23]. In LandScan, the brightness of nighttime lights is used to calculate weight coefficients of population distribution of individual cells, but in addition to the brightness of nighttime lights, many other factors (e.g., land cover, slope, and distance to roads) also impact the weight coefficients [25]. Moreover, changes of population counts of individual cells are primarily determined by changes of total population of the administrative units where the individual cells are located. The total population of each administrative unit is obtained by census.

Supporting data of GDP growth rates that were used to evaluate reliability of the processed NLT images were taken from the World Bank [26].

## III. METHODOLOGY

DN values in NLT image products are incompatible among different individual image products and across different years. Fig. 1 exhibits sum lights of China and the U.S. derived from NLT image products. In most years, two DMSP satellites collect global data separately, and thus, two corresponding

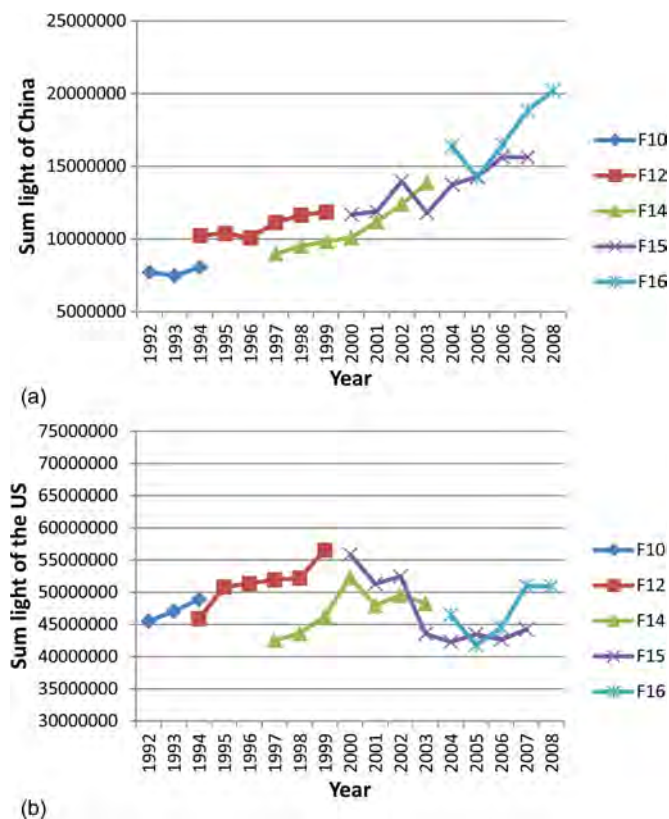


Fig. 1. Sum lights of (a) China and (b) the U.S. derived from original NLT image products.

image products are usually produced for the same year. It may be expected that, if DN values in NLT image products were compatible, sum lights derived from two different satellite image products for the same year should be almost the same. However, the reality is that apparent differences in sum lights exist between images collected by different satellites for the same year. For example, sum lights derived from satellite F12-collecting image products are markedly larger than those derived from F14-collecting image products for 1997, 1998, and 1999 (see Fig. 1). Additionally, sum lights derived from NLT image products lack continuity with abnormal fluctuations in sum light emerging for the same satellite across different years. For example, sum light derived from F16-collecting image products is abnormally large in 2004 (see Fig. 1). It cannot be guaranteed that variations in DN value across different years are caused by changes in brightness of nighttime lights or gain value of sensors [6], [27]. In addition to the problems of incompatible and discontinuous DN values, geographic inconsistencies widely exist among NLT image products. Fig. 2(a) provides an example showing the geographic inconsistencies in which 1-pixel geometric difference in vertical direction exists between images from 2004 collected by satellites F15 and F16. Therefore, before using NLT image products for a quantitative multiyear study, it is necessary to execute the present study methods by intercalibrating DN values and correcting geometric errors in the NLT image products.

The main steps of correcting the DN values and geometric errors in the NLT image products are exhibited in Fig. 3. We first used the approach of Elvidge *et al.* [2] to develop a

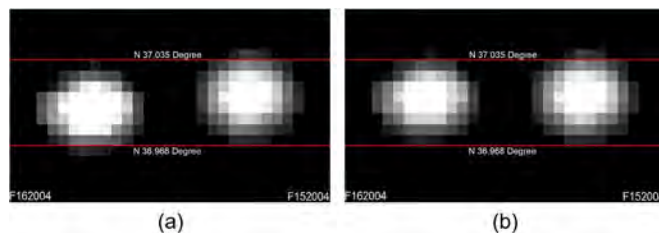


Fig. 2. (a) Example showing geometric errors in NLT images. One lit area has different geographic positions in images in 2004 collected by satellites F15 and F16. (b) Geometrically corrected positions of the lit area in images collected by satellites F15 and F16 in 2004.

group of second-order functions to intercalibrate NLT image products. Second, we selected an intercalibrated image collected by DMSP satellite F14 in 2001 as a reference image and conducted geometric corrections for the intercalibrated NLT images by seeking the largest coefficients of correlation between the reference image and the shifted candidate images. Third, we improved the method of Liu *et al.* [5] (i.e., supposing a pixel’s DN value in an early NLT image should not be larger than its DN value in a later NLT image) to adjust intercalibrated NLT images twice with different orders of adjustment. In the first adjustment, the intercalibrated NLT images were adjusted sequentially from 2008 to 1992, and in the second adjustment, the intercalibrated NLT images were adjusted sequentially from 1992 to 2008. We averaged the first and the second adjusted NLT images to partly avoid largely under- or over-valuation for the earliest (e.g., 1992, 1993, and 1994) and the latest (e.g., 2008, 2007, and 2006) images. Fourth, we employed gridded population to correct DN values in the adjusted NLT images. If a pixel’s population did increase, we retained its DN values on the adjusted NLT images; otherwise, we restored the pixel’s DN values to those on the intercalibrated NLT images.

### A. Intercalibration

Using the method of Elvidge *et al.* [2], the 1999 annual image composite collected by F12 was selected as a baseline reference image and Sicily, Italy was supposed to be a region with little nighttime light change from 1992 and 2008. A group of quadratic polynomial regression equations (see Table I) was developed by adjusting DN values of pixels in the region of Sicily in candidate NLT image products to match DN values of pixels in the region of Sicily in the reference image. The regression equations were applied to their corresponding original NLT image products, respectively, to build intercalibrated NLT images.

Many unlit pixels in original NLT image products have nonzero DN values due to the existence of background noise. Moreover, after intercalibration, pixels with DN value of 0 in original NLT image products have nonzero DN values because nonzero constants in quadratic polynomial regression equations were added to the pixels. To obtain reliable lit area and sum light information, a threshold is needed to process these pixels. In the other type of NLT image subproducts (i.e., average DN value image composites) where background noise has been removed and DN values are integers, the smallest DN value for lighted pixels is 3. (There is no pixel with DN value of 1

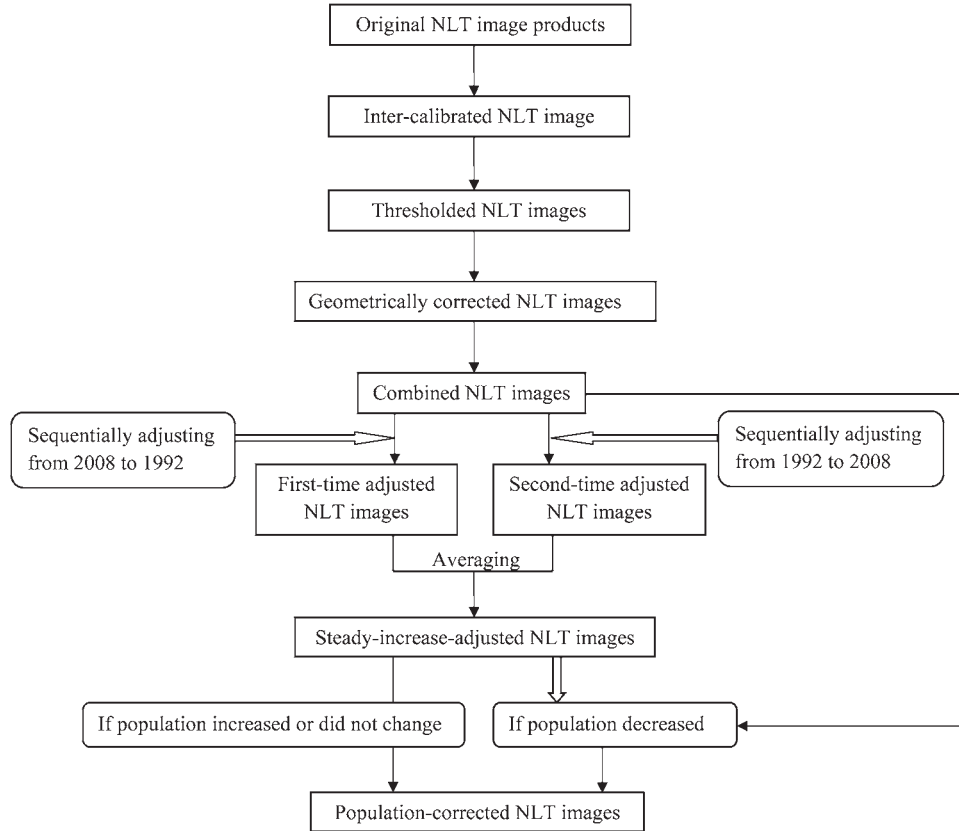


Fig. 3. Flowchart for correcting incompatible DN values and geometric errors.

TABLE I  
REGRESSION FUNCTIONS FOR INTERCALIBRATING THE NLT IMAGE PRODUCTS. INTERCALIBRATED DN VALUE ( $DN_{intercalibrated}$ ) IS CREATED BY THE APPLICATION OF THIS FUNCTION:  
 $DN_{intercalibration} = \beta_0 + \beta_1 \times DN + \beta_2 \times DN^2$

Satellite	Year	$\beta_0$	$\beta_1$	$\beta_2$	$R^2$
F10	1992	-0.06330	1.44742	-0.00711	0.9291
F10	1993	-0.16357	1.52471	-0.00822	0.9509
F10	1994	-0.01449	1.45547	-0.00744	0.9486
F12	1994	0.05653	1.13210	-0.00194	0.9398
F12	1995	0.14178	1.23096	-0.00390	0.9443
F12	1996	0.06061	1.28073	-0.00431	0.9537
F12	1997	0.00583	1.16339	-0.00246	0.9482
F12	1998	0.00461	1.05529	-0.00115	0.9694
F12	1999	0	1	0	1
F14	1997	0.06917	1.69215	-0.01115	0.9387
F14	1998	0.04814	1.61247	-0.00985	0.9809
F14	1999	-0.04959	1.48937	-0.00756	0.9801
F14	2000	0.17751	1.38101	-0.00621	0.9506
F14	2001	-0.05976	1.32240	-0.00503	0.9603
F14	2002	0.09352	1.22957	-0.00402	0.9462
F14	2003	-0.15229	1.27187	-0.00417	0.9593
F15	2000	0.08490	1.04873	-0.00108	0.9545
F15	2001	-0.15960	1.06120	-0.00056	0.9705
F15	2002	-0.13117	0.95000	0.00115	0.9757
F15	2003	-0.06442	1.51146	-0.00784	0.9506
F15	2004	-0.13613	1.34659	-0.00512	0.9640
F15	2005	-0.21526	1.30007	-0.00421	0.9531
F15	2006	-0.21407	1.31066	-0.00429	0.9565
F15	2007	0.06909	1.36229	-0.00535	0.9301
F16	2004	-0.07121	1.17645	-0.00294	0.9362
F16	2005	-0.05247	1.39633	-0.00594	0.9569
F16	2006	0.77279	1.12778	-0.00150	0.9441
F16	2007	0.07830	0.93757	0.00106	0.9640
F16	2008	-0.09108	1.00312	0.00003	0.9617

or 2 in China and the U.S.) We assumed that DN values smaller than 3 and equal to or larger than 2.5 have been rounded to 3 in the average DN value image composites, and consequently, any pixel with stable nighttime lights (i.e., anthropogenic lights from cities, towns, and other sites with persistent lighting) should have a DN value equal to or larger than 2.5 in the intercalibrated NLT images; hence, pixels in the intercalibrated annual images were thresholded by (1) that guarantees all unlit pixels in original NLT image products have DN value of 0 in intercalibrated images

$$DN_{thresholded} = \begin{cases} 0, & DN_{inter} < 2.5 \\ DN_{inter}, & DN_{inter} \geq 2.5 \end{cases} \quad (1)$$

where  $DN_{inter}$  is the DN value in the intercalibrated NLT images.

After intercalibration, compatibility and continuity of the NLT image data were greatly improved as indicated by the markedly reduced differences in sum light between two satellites for the same year (see Fig. 4). Additionally, fluctuations in sum light across different years were also reduced (see Fig. 4). However, DN values in the intercalibrated NLT images are still not completely compatible and continuous. For example, a relatively large discrepancy still exists between satellites F10 and F12 in 1994 (see Fig. 4). Additionally, an abnormal increase in sum light in the U.S. derived from the F14-collected image emerges in 2000 (see Fig. 4). Hence, the intercalibrated NLT image data need to be further improved.

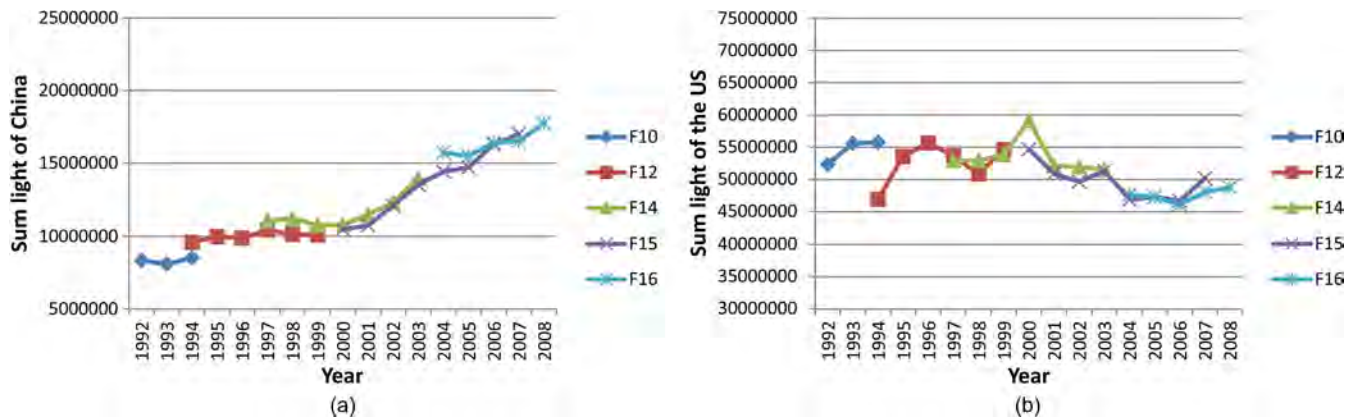


Fig. 4. Sum lights of (a) China and (b) the U.S. derived from intercalibrated NLT images.

TABLE II  
MOVEMENT SCHEMATA OF GEOMETRIC CORRECTION FOR CHINA AND THE U.S.

Year	Satellite	China			The US		
		Movement scheme	Original correlation	Largest correlation	Movement scheme	Original correlation	Largest correlation
1992	F10	None	0.8959	0.8959	None	0.9719	0.9719
1993	F10	Left one	0.9026	0.9055	Up one & left one	0.9651	0.9693
1994	F10	None	0.9120	0.9120	Up one	0.9623	0.9627
1994	F12	Up one	0.9219	0.9241	Up one	0.9747	0.9765
1995	F12	Up one	0.9348	0.9380	Up one	0.9762	0.9803
1996	F12	Up one	0.9369	0.9450	Up one	0.9780	0.9835
1997	F12	Up one	0.9470	0.9524	Up one	0.9765	0.9848
1998	F12	None	0.9596	0.9596	Up one	0.9830	0.9833
1999	F12	left one	0.9639	0.9666	left one	0.9824	0.9846
1997	F14	Up one	0.9388	0.9460	Up one	0.9789	0.9844
1998	F14	Left one	0.9543	0.9590	Left one	0.9852	0.9875
1999	F14	None	0.9643	0.9643	None	0.9881	0.9881
2000	F14	None	0.9772	0.9772	None	0.9848	0.9848
2001	F14	None	1	1	None	1	1
2002	F14	Up one	0.9691	0.9752	Up one	0.9814	0.9881
2003	F14	None	0.9627	0.9627	None	0.9879	0.9879
2000	F15	Up one & left one	0.9672	0.9759	Up one & left one	0.9806	0.9863
2001	F15	Left one	0.9750	0.9829	Left one	0.9886	0.9931
2002	F15	Left one	0.9662	0.9722	Left one	0.9870	0.9881
2003	F15	Up one & left one	0.9510	0.9541	Left one	0.9872	0.9877
2004	F15	None	0.9471	0.9471	None	0.9868	0.9868
2005	F15	Up one & left one	0.9308	0.9425	Left one	0.9826	0.9835
2006	F15	None	0.9328	0.9328	None	0.9814	0.9814
2007	F15	None	0.9259	0.9259	Right one	0.9778	0.9801
2004	F16	Up one & left one	0.9386	0.9492	Up one	0.9797	0.9865
2005	F16	None	0.9451	0.9451	None	0.9862	0.9862
2006	F16	None	0.9296	0.9296	None	0.9782	0.9782
2007	F16	None	0.9261	0.9261	None	0.9818	0.9818
2008	F16	Left one	0.9135	0.9147	None	0.9772	0.9772

B. Geometric Correction

Liu *et al.* [5] found that some lit pixels in an intra-annual image are not necessarily lit in another one; thus, they consequently treated the pixels as unstably lit pixels and revalued them as 0. However, Liu *et al.* [5] selected average DN value image composites in which unstable lights have been mostly removed [2]. Disappearance of some lit pixels in an intra-annual image may be partly due to geometric errors. It is shown in Fig. 2(a) that a 1-pixel geometric difference in vertical direction exists between images from 2004 collected by satellites F15

and F16. When the two images are overlaid, lit pixels in the F162004 image under the lower red line (the line of N 36.968°) were not lit in the F152004 image [see Fig. 2(a)]. Thus, it is necessary to execute geometric corrections for the intercalibrated NLT images.

We used a shift-based method to perform the geometric corrections with guarantee that DN values in the NLT images are unchanged. The 2001 image collected by F14, in the middle of the list of the NLT series, was arbitrarily selected as a reference image. With each intercalibrated NLT image overlaid on the reference image, a correlation coefficient of DN values

between the two images was calculated. Then, the annual image was moved horizontally (left or right), vertically (up or down), or horizontally and vertically simultaneously from 0 to 2 pixels each time. Correlation coefficients of the DN values between the moved annual image and the reference image were calculated. There are 25 possible movement combinations, including that one is for none in either direction. It can be expected that the largest correlation coefficient should emerge when geographic positions of each couple of pixels derived from the two images are the closest. Thus, the annual image was shifted according to a movement schema in which the largest correlation coefficient emerged. The above process of geometric correction was performed for each annual image in China and the U.S. to obtain geometrically corrected NLT images. Table II exhibits the movement schemata of the geometric corrections for China and the U.S., respectively. Fig. 4(b) shows geometrically corrected position of the lit area where a 1-pixel geometric difference in vertical direction existed.

If two geometrically corrected images (collected by different satellites) exist for the same year, the two images were combined by averaging their DN values. Sum lights of China and the U.S. derived from the combined geometric correction images are shown in Fig. 5.

C. Adjustment Based on the Assumption of Steady Increases in DN Value

To further improve compatibility and continuity of intercalibrated NLT image data, Liu *et al.* [5] assumed that deurbanization did not exist in China from 1992 to 2008; hence, consequently, decreases in lit area and DN values of pixels should not exist in nighttime lights images. In this paper, we adapted the method of Liu *et al.* [5] to adjust DN values of NLT images in China and the U.S. All annual images were adjusted by (2) to guarantee that DN value of each pixel in an early annual image is not larger than that in a later annual image

$$DN_{(y,i)} = \begin{cases} DN_{(y+1,i)}, & DN_{(y,i)} > DN_{(y+1,i)} \\ DN_{(y,i)}, & DN_{(y,i)} \leq DN_{(y+1,i)} \end{cases} \quad (2)$$

where *i* represents the *i*th pixel in a nighttime light image, and *y* represents a year between 1992 and 2007. While after the adjustment, DN value of each pixel in the 2008 annual image did not experience any changes, DN values of some pixels in earlier annual images might be reduced. DN values of pixels in earlier annual (e.g., 1992, 1993, and 1994) images are more likely reduced largely, and it may lead to early annual images' DN values being smaller than their actual DN values (see Fig. 6). Thus, we performed a second steady-increase adjustment.

In the second steady-increase adjustment, we reversed the order of adjustment and used (3) to guarantee that DN value of each pixel in a later annual image is not smaller than that in an early annual image

$$DN_{(y,i)} = \begin{cases} DN_{(y-1,i)}, & DN_{(y,i)} < DN_{(y-1,i)} \\ DN_{(y,i)}, & DN_{(y,i)} \geq DN_{(y-1,i)} \end{cases} \quad (3)$$

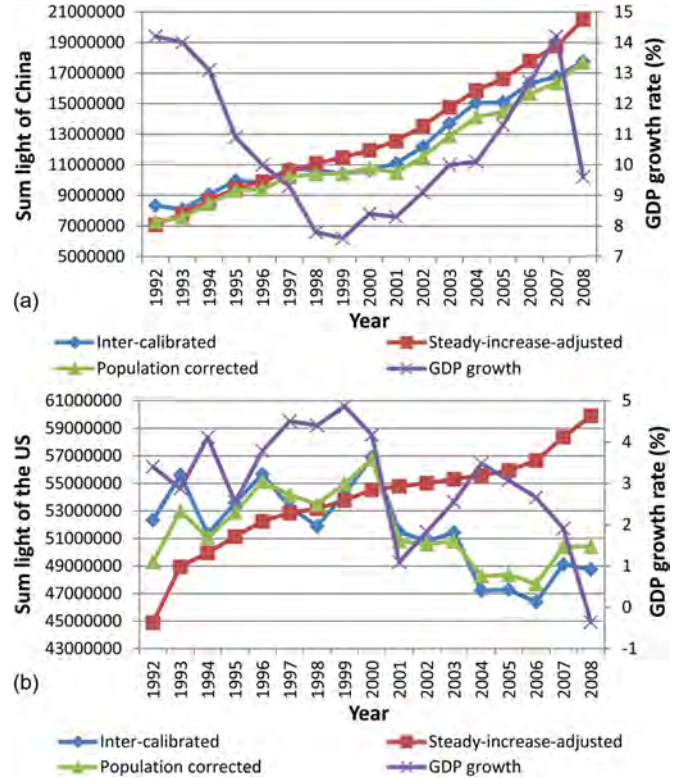


Fig. 5. GDP growth rates and annual sum lights of (a) China and (b) the U.S. derived from intercalibrated (and combined), steady-increase-adjusted, and population-corrected NLT images.

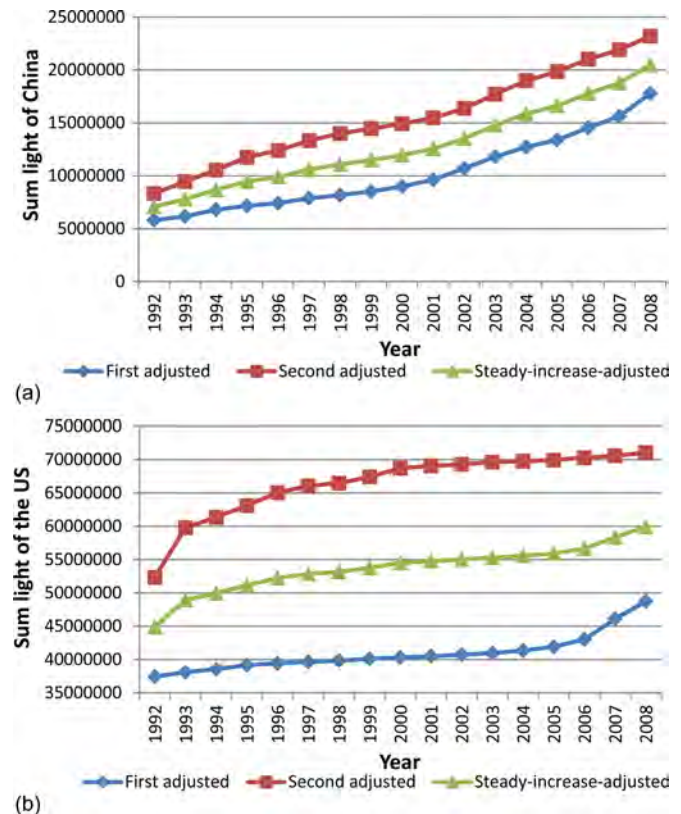


Fig. 6. Annual sum lights of (a) China and (b) the U.S. derived from the first interannual revalued, the second interannual revalued, and the averaged interannual revalued NLT images.

where  $i$  represents the  $i$ th pixel in a nighttime light image, and  $y$  represents a year between 1993 and 2008. This reversal of the order of adjustment avoided DN values of pixels in earlier annual images that were largely reduced but led to DN values of pixels in later annual (e.g., 2008, 2007, and 2006) images that were excessively enlarged (see Fig. 6). To make adjusted DN values close to their actual DN values, we averaged the first and the second steady-increase-adjusted images to obtain steadily increasing DNs in NLT images.

#### D. Correction With Population Data

From 1992 to 2008, most Chinese areas experienced high economic and urban population growth with rare deurbanization [14]. Consequently, the assumption that DN value of each pixel in an early/late annual image is not larger or smaller than that in a later/earlier annual image per the work of Liu *et al.* [5] seems appropriate for China. However, during the same period, urban decline widely emerged in the U.S., particularly in post-industrial cities such as Chicago, Detroit, and Philadelphia [10]. Decline of traditional industries (e.g., steel and automobile manufacturing) in such cities has led to large losses in urban population. Moreover, a large number of people moved to suburbs to enjoy better quality of life environment and avoid high housing costs and high crime rates in many urban centers [7], [8], [28]–[30]. With the decrease in the U.S. urban population, the number of local businesses declined, and consequently, brightness of nighttime lights decreased. Hence, simply applying the assumption of steady increase in DN value may produce errors in the U.S. because brightness of nighttime lights does not always increase in a considerable number of places. In this paper, we employed gridded population data derived from GRUMP's population density grid data set (for years 1990, 1995, and 2000) and LandScan population data set (for year 2008) to further improve NLT image data. Previous studies have shown that brightness of nighttime light strongly correlated to population density [31]–[33]. Our basic correcting schema is that, if during a certain period, population increases in a region, business and brightness of nighttime lights should also increase in the region. Then, we applied the assumption of steady increases in DN value. If during a certain period, population does not increase, we assumed that DN values in intercalibrated NLT images before revaluation reflect changes in brightness of actual nighttime lights reasonably; thus, we restored DN values to those on the intercalibrated (and thresholded) NLT images. Specifically, DN values on the averaged interannual revalued NLT images were corrected by (4) as follows:

$$\begin{aligned} & \text{DN}_{\text{corrected}}^y \\ &= \begin{cases} \text{DN}_{\text{revalued}}^y, & \text{if } P_i^{t_j} < P_i^{t_{j+1}} \\ \text{DN}_{\text{inter}}^y, & \text{if } P_i^{t_j} \geq P_i^{t_{j+1}} \end{cases} \quad (t_j < y \leq t_{j+1}, 1 \leq j \leq 3) \end{aligned} \quad (4)$$

where  $P$  represents population,  $\text{DN}_{\text{revalued}}$  is the DN value on NLT images revalued by the supposition of steady increases in DN value,  $\text{DN}_{\text{inter}}$  is the DN value on intercalibrated (and

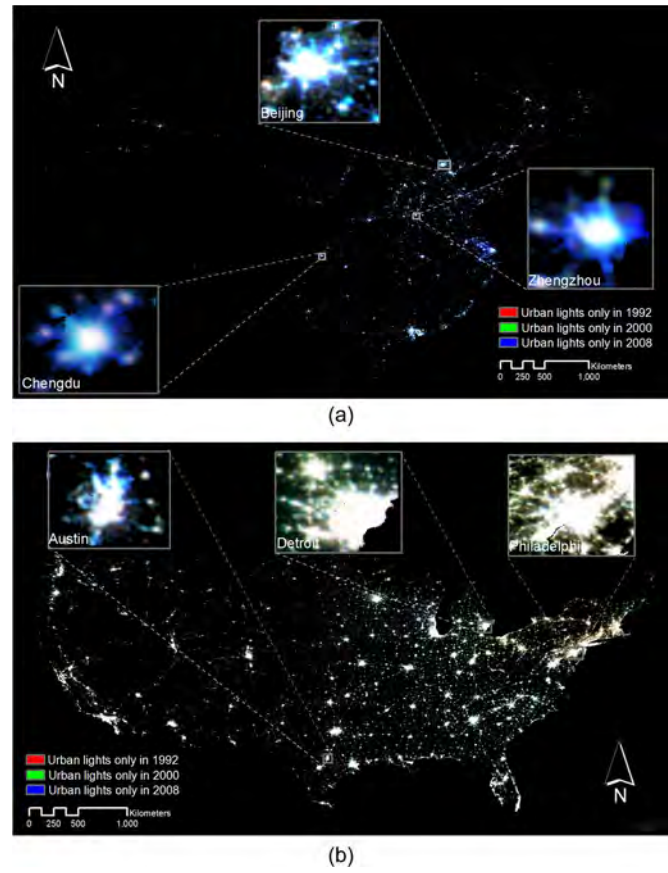


Fig. 7. Nighttime lights development/decay in (a) China and (b) the U.S., respectively, derived from population-corrected nighttime light images.

thresholded) NLT images,  $\text{DN}_{\text{corrected}}$  is the DN value on final corrected NLT images,  $i$  represents the  $i$ th pixel,  $y$  represents a year of the NLT images (i.e., 1992, 1993, ..., 2008),  $t$  represents a year of available gridded population data, and  $j$  represents the  $j$ th obtained gridded population data (i.e.,  $t_1 = 1990$ ,  $t_2 = 1995$ ,  $t_3 = 2000$ , and  $t_4 = 2008$ ). Hereafter, the NLT images corrected by the population data were referred to as population-corrected NLT images.

#### E. Analyses and Exhibition of Nighttime Lights Development/Decline

Sum light and lit area are the most used physical measures derived from nighttime light images to assess urban development and socioeconomic factors [12], [27], [34], [35]. Sum light not only indicates a region's total brightness of nighttime lights but also suggests variables of population and economy of the region [18]. Lit areas have been traditionally treated as developed areas where a number of stable socioeconomic activities exist and unlit areas have been treated as undeveloped areas where stable socioeconomic activities rarely occur [36]. Developed areas can be further divided into urban and suburban areas through setting thresholds of DN value [11], [36], [37]. Additionally, lit area can be also treated as a measure of socioeconomic factors at the national or the regional scales [35], [38]. Thus, in this paper, we used sum light and lit area to evaluate nighttime lights development/decay in China and

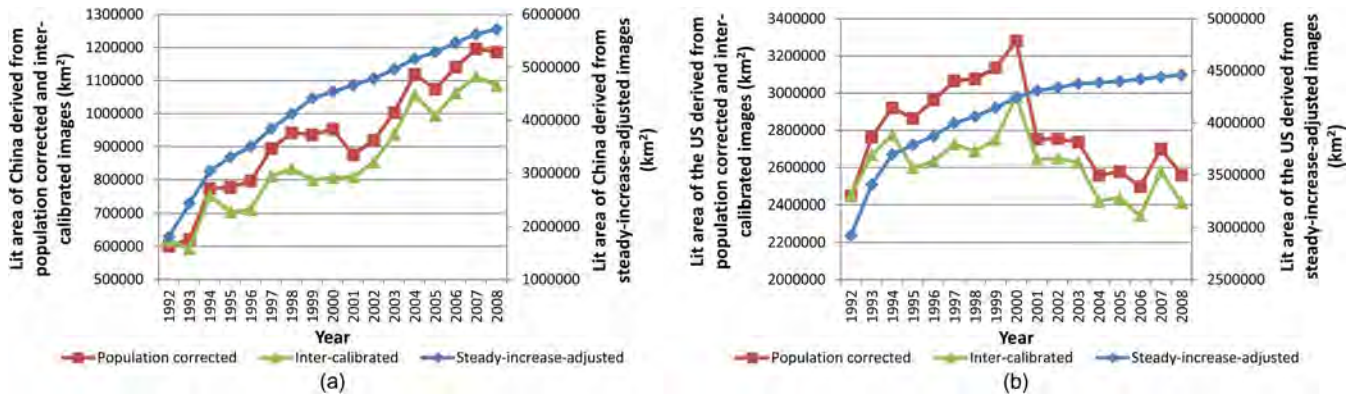


Fig. 8. Lit areas of (a) China and (b) the U.S. derived from population-corrected, intercalibrated (and combined), and steady-increase-adjusted NLT images.

the U.S. To exhibit spatiotemporal changes of nighttime lights in China and the U.S., two false color maps were produced by overlaying three population-corrected nighttime light images of 1992, 2000, and 2008 (see Fig. 7).

#### IV. RESULTS AND DISCUSSION

##### A. Evaluation of Corrected NLT Data

It is not surprising that, after adjusting DN values with assumption of steadily increasing DN value, sum lights of China and the U.S. both exhibit continuous increases across years (see Fig. 6). By contrast, sum lights derived from population-corrected NLT images did not show a continuously increasing trend (see Fig. 5). Specifically, from 1992 to 2008, changes of sum light in China can be divided into three phases. In the first phase, 1992–1997, sum light in China increases at high rates. During the second phase, 1998–2001, sum light data in China are nearly unchanged, and in 2001, a small decrease in sum light occurs. In the third phase, 2002–2008, sum light in China dramatically increases again [see Fig. 5(a)]. From 1992 to 2008, changes of sum light in the U.S. can be divided into two phases. The first phase, 1992–2000, exhibits overall changing tendency of sum light in the U.S. that is increasing. During the second phase, 2001–2008, the overall changing tendency of sum light in the U.S. is decreasing with decrease bottoming out in 2006 and small increases in sum light emerging through 2008 [see Fig. 5(b)].

Brightness of nighttime lights is a good indicator for a country's or a region's economic changes [1], [16], [39], [40]. Although the sum lights derived from steady-increase-adjusted NLT images are more continuous than those derived from population-corrected NLT images spanning the period of 1992–2008, changes in sum light derived from population-corrected NLT images are more temporally consistent with changes in economy than those derived from steady-increase-adjusted NLT images. Specifically, the 17-year period of 1992–2008 for China can be also divided into three phases based on rates of China's economic development. The first phase is from 1992 to 1997 in which China experienced rapid economic growth with GDP growth rates larger than 9%. The second phase is from 1998 to 2001 when China experienced relatively small economic growth with GDP growth rates larger

than 7% and smaller than 9%. The third phase is from 2002 to 2008 in which China's economy rapidly developed again with GDP growth rates larger than 9% [see Fig. 5(a)]. The 17 years for the U.S. can be divided into two phases dependent on rates of economic development of the U.S. In the first phase, 1992–2000, the U.S. experienced relatively rapid economic growth with GDP growth rates greater than 3%. During the second phase, from 2001 to 2008, economic growth of the U.S. slowed. In most years of the second phase, GDP growth rates are smaller than 3% [see Fig. 5(b)].

It can be expected that, if a country does not experience any severe circumstance, such as political unrest, economic collapse, or natural catastrophe, its economy will not exhibit drastic change and sum light should steadily change relative to the year before. Compared with sum light derived from intercalibrated NLT images, sum light derived from population-corrected NLT images has small fluctuations and steady increases/decreases across years. For example, from 1992 to 2000, the overall changing tendency of sum light in the U.S. is increasing. However, intercalibrated NLT data show that a sharp decrease exists during 1996–2000 [see Fig. 5(b)]. After further population correction, the sharp decrease becomes smooth. Additionally, in 1992 and 1993, China experienced large economic growth with GDP growth rates of approximately 14%. However, intercalibrated NLT data show a decrease in sum light in China from 1992 to 1993 that is very abnormal and questionable [see Fig. 5(a)]. After population correction, this decrease has been replaced by a steady increase. Thus, population-corrected NLT imagery data have better continuity than intercalibrated NLT imagery data.

Changes of sum light derived from population-corrected NLT images are relatively volatile, but the fluctuations are temporally consistent with the changes in the economy and, consequently, can represent brightness of nighttime lights on the ground more accurately. Additionally, some sharp or abnormal changes in sum light still exist after NLT images are intercalibrated. However, with further population correction, such sharp changes are smoothed and such abnormal changes have disappeared. Thus, the method developed in this paper does not only improve compatibility and continuity of NLT image data but also amplify accuracy of NLT image data to reflect brightness of nighttime lights on the ground.

TABLE III  
DIFFERENCES BETWEEN GRUMP AND LANDSCAN

Gridded population data set	Census data	Approach	DN value	Uses of nighttime lights
GRUMP	Obtained at the administrative unit level (mostly at the city level)	Census data centered: population data for settlements from census data	Average population counts over a 24-hour period	delimiting areal extents of human settlements
Landscan	Mostly obtained at the province level	Remotely sensed data centered: population data for settlements from estimations based on weight coefficients which are calculated by factors (e.g. land cover, slope, and nighttime lights) derived from remote sensing imagery	Population counts at residences	As one of factors to estimate weight coefficients

### B. Spatiotemporal Characteristics of Nighttime Lights Development/Decay in China and the U.S.

After the population correction China's lit area and sum light generally kept growing from 1992 to 2008, but large variances in the growth rates of the lit area and the sum light exist among different time intervals [see Figs. 5(a) and 8(a)]. During the five years between 1992 and 1997, China's lit area increased 48.95%, an average annual increase rate of 9.79%, and sum light increased 40.4%, an average annual increase rate of 8.09%. From 1998 to 2000, the speed of Chinese nighttime lights development apparently slowed with annual increase rates of lit area and sum light of only 2.19% and 1.93%, respectively. Moreover, in 2001, Chinese lit area and sum light fell back to 1997 levels [see Figs. 5(a) and 8(a)]. After 2001, China's lit area and sum light rapidly increased again. During the seven years between 2002 and 2008, China's lit area increased 35.53%, an average annual increase rate of 5.08%, and sum light increased 68.84%, an average annual increase rate of 9.83%. Therefore, although positive development is an overall trend for most Chinese areas from 1992 to 2008, stalled development and even small decay in nighttime lights still emerged in China during the relatively short period of 1998–2001.

Since 1992, lit area and sum light in the U.S. increased with average annual increase rates of 4.25% and 1.89%, respectively, and reached peak values in 2000. After slowing of economic growth in 2000, lit area and sum light in the U.S. began to decrease, and in 2006, it fell back to the levels of 1992 [see Figs. 5(b) and 8(b)]. After 2006, GDP growth rates in the U.S. are still very small and even negative in 2008, but lit area and sum light in the U.S. began to rebound slightly in these years [see Figs. 5(b) and 8(b)]. Thus, from 1992 to 2008, the U.S. experienced small annual positive nighttime lights development within a large fluctuation of nighttime lights development for the whole period.

The false color maps [see Fig. 7(a) and (b)] more clearly show spatiotemporal patterns of nighttime lights development/decline in China and the U.S., respectively. In most Chinese cities, nighttime lights showed apparent development trends. Specifically, three circles can be found for major Chinese cities in Fig. 7(a). The inner circles (white color) are established developed areas where nighttime lights can be observed in all three years (i.e., 1992, 2000, and 2008). The middle circles (cyan color) are newly developed areas emerged after 2000

where nighttime lights can be observed between 2000 and 2008. The outer circles (blue color) are newly developed areas emerging after 2007 where nighttime lights can be only observed in 2008.

Two circles can be found for most northern cities of the U.S. [see Fig. 7(b)]. The inner circles (white color) are established developed areas in three periods. The outer circles show green or red-brown color. The green color indicates that nighttime lights can be only observed in 2000, and the red-brown color suggests that nighttime lights can be observed clearly in 1992 and 2000 but observed dimly in 2008. These circles demonstrate that, before 2000, nighttime lights in most northern areas of the U.S. increased, but after 2000, they declined. In addition to the aforementioned two circles, some southern cities of the U.S. (e.g., Dallas, Austin, Atlanta, and Orlando) had some regions with blue or cyan color, which suggests that nighttime lights development occurred in the cities after 2000.

## V. CONCLUSION

In this paper, we have proposed methods to explore and reduce geometric errors in NLT image products through seeking out the largest correlation coefficient of DN values between a reference image and a candidate image. We find that, when the 2001 image collected by F12 was selected as a reference image, 16 of 29 NLT image products for China and 18 of 29 NLT image products for the U.S. have one or two pixel geometric errors. Moreover, we improve previous methods (i.e., Elvidge *et al.* [2] and Liu *et al.* [5]) and used population data to further improve NLT image data. The NLT data adjusted by the methodology of this paper are more continuous than those intercalibrated by the method of Elvidge *et al.* [2] and more accurately represent brightness of nighttime light on the ground than those corrected by the method of Liu *et al.* [5]. Specifically, DN values in the corrected NLT images of this paper have relatively small abnormal fluctuations across different years, and the changes in DN value temporally coincide with the changes in GDP growth rate.

Through analyzing the population-corrected NLT image data, we find that nighttime lights development is not linear in either China or the U.S. Fluctuation, stagnation, and decay existed across the process of nighttime lights development in China and the U.S. From 1992 to 2008, Chinese nighttime lights experienced two rapid development periods (i.e.,

1992–1997 and 2001–2008). Between these periods, nighttime lights development is nearly stagnant and even retrogressive. From 1992 to 2001, nighttime lights in the U.S. showed an apparently increasing trend. However, after 2001, with a slow-down in economic growth, most areas in the U.S. experienced continuous nighttime lights decay until 2006.

The population-corrected NLT data with better compatibility, continuity, and accuracy can be used as measures of multiyear changes of socioeconomic factors (e.g., GDP, electric power consumption, and fossil fuel carbon dioxide emission). Moreover, due to the correction of geometric errors, the population-corrected NLT data are particularly appropriate for studies regarding urban landscape and urbanization that have relatively high requirements for data's geometric accuracy. In the future, we will use the population-corrected NLT data to assess and project urbanization and changes of urban economy and population in China and the U.S.

As a final caveat, the GRUMP DN values represent population counts directly disaggregated from census administrative units, yet in the LandScan data, mobility of population is considered; hence, DN values represent average population counts over a 24-h period [25]. Consequently, DN values of GRUMP and LandScan are not completely consistent. (Detailed differences between the GRUMP and the LandScan have been shown in the appendix table.) Neither the GRUMP nor the LandScan data sets can cover the whole study period (i.e., from 1992 to 2008); hence, we used the GRUMP and the LandScan sets jointly. We remind future users of this method that this limitation of the joint use of GRUMP and the LandScan population data sets may produce unforeseen errors on corrected DN values in nighttime light images.

#### APPENDIX

See Table III for details.

#### ACKNOWLEDGMENT

The authors would like to thank three anonymous reviewers for their constructive comments and the many colleagues and organizations that shared data used in this paper.

#### REFERENCES

- [1] X. Chen and W. D. Nordhaus, "Using luminosity data as a proxy for economic statistics," *Proc. Nat. Academy Sci. USA*, vol. 108, no. 21, pp. 8589–8594, 2010.
- [2] C. D. Elvidge *et al.*, "A fifteen year record of global natural gas flaring derived from satellite data," *Energies*, vol. 2, no. 3, pp. 595–622, Aug. 2009.
- [3] C. D. Elvidge *et al.*, "Area and position accuracy of DMSP nighttime lights data," in *Remote Sensing and GIS Accuracy Assessment*, R. S. Lunetta and J. G. Lyon, Eds. London, U.K.: CRC Press, 2004, pp. 281–292.
- [4] B. Tuttle, S. J. Anderson, P. C. Sutton, C. D. Elvidge, and K. Baugh, "It used to be dark here: Geolocation calibration of the Defense Meteorological Satellite Program Operational Linescan System," *Photogramm. Eng. Remote Sens.*, vol. 79, no. 3, pp. 287–297, 2013.
- [5] Z. Liu, C. He, Q. Zhang, Q. Huang, and Y. Yang, "Extracting the dynamics of urban expansion in China using DMSP-OLS nighttime light data from 1992 to 2008," *Landscape and Urban Planning*, vol. 106, no. 1, pp. 62–72, May 2012.
- [6] N. Zhao, T. Ghosh, and E. L. Samson, "Mapping spatio-temporal changes of Chinese electric power consumption using night-time imagery," *Int. J. Remote Sens.*, vol. 33, no. 20, pp. 6304–6320, 2012.
- [7] T. Rieniets, "Shrinking cities: Causes and effects of urban population losses in the twentieth century," *Nature Culture*, vol. 4, no. 3, pp. 231–254, 2009.
- [8] E. L. Glaeser and J. Gyourko, "Urban decline and durable housing," *J. Political Econ.*, vol. 113, no. 2, pp. 345–375, 2005.
- [9] J. B. Cullen and S. D. Levitt, "Crime, urban flight, and the consequences for cities," *The Review of Economics and Statistics*, vol. 81, no. 2, pp. 159–169, May 1999.
- [10] P. A. Simmons and R. E. Lang, *The Urban Turnaround: A Decade-by-Decade Report Card on Postwar Population Change in Older Industrial Cities*. Washington, DC, USA: The Fannie Mae Foundation, 2001.
- [11] C. Small, F. Pozzi, and C. D. Elvidge, "Spatial analysis of global urban extent from DMSP-OLS night lights," *Remote Sens. Environ.*, vol. 96, no. 3/4, pp. 277–291, Jun. 2005.
- [12] Q. Zhang and K. C. Seto, "Mapping urbanization dynamics at regional and global scales using multi-temporal DMSP/OLS nighttime light data," *Remote Sens. Environ.*, vol. 115, no. 9, pp. 2320–2329, Sep. 2011.
- [13] X. Cao, J. Chen, H. Imura, and O. Higashi, "A SVM-based method to extract urban areas from DMSP-OLS and SPOT VGT data," *Remote Sens. Environ.*, vol. 113, no. 10, pp. 2205–2209, Oct. 2009.
- [14] T. Ma, C. Zhou, T. Pei, S. Haynie, and J. Fan, "Quantitative estimation of urbanization dynamics using time series of DMSP/OLS nighttime light data: A comparative case study from China's cities," *Remote Sens. Environ.*, vol. 124, pp. 99–107, Sep. 2012.
- [15] W. Wang, H. Cheng, and L. Zhang, "Poverty assessment using DMSP/OLS night-time light satellite imagery at a provincial scale in China," *Adv. Space Res.*, vol. 49, no. 8, pp. 1253–1264, Apr. 2012.
- [16] N. Zhao, N. Currit, and E. Samson, "Net primary production and gross domestic product in China derived from satellite imagery," *Ecol. Econ.*, vol. 70, no. 5, pp. 921–928, Mar. 2011.
- [17] J. Wu, Z. Wang, W. Li, and J. Peng, "Exploring factors affecting the relationship between light consumption and GDP based on DMSP/OLS nighttime satellite imagery," *Remote Sens. Environ.*, vol. 134, pp. 111–119, Jul. 2013.
- [18] P. C. Sutton, C. D. Elvidge, and T. Ghosh, "Estimation of gross domestic product at sub-national scales using nighttime satellite imagery," *Int. J. Ecol. Econ. Statist.*, vol. 8, no. SO7, pp. 5–21, 2007.
- [19] C. D. Elvidge, F. Hsu, K. E. Baugh, and T. Ghosh, "National trends in satellite-observed lighting 1992–2012," in *Global Urban Monitoring and Assessment Through Earth Observation*, Q. Weng, Ed. London, U.K.: CRC Press, 2014, pp. 97–120.
- [20] Q. Zhang, C. He, and Z. Liu, "Studying urban development and change in the contiguous United States using two scaled measures derived from nighttime lights data and population census," *GISci. Remote Sens.*, vol. 51, no. 1, pp. 63–82, 2014.
- [21] K. Baugh, C. Elvidge, T. Ghosh, and D. Ziskin, "Development of a 2009 Stable Lights Product using DMSP-OLS data," in *Proc. 30th Asia-Pacific Adv. Netw. Meet.*, 2010, pp. 114–130.
- [22] Center for International Earth Science Information Network (CIESIN)/Columbia University, International Food Policy Research Institute (IFPRI), The World Bank, Centro Internacional de Agricultura Tropical (CIAT), *Global Rural-Urban Mapping Project, Version 1 (GRUMPv1): Population Density Grid. Palisades, NY: NASA Socioeconomic Data and Applications Center (SEDAC)*, 2011 (Last accessed January 24, 2014). [Online]. Available: <http://sedac.ciesin.columbia.edu/data/set/grump-v1-population-density>
- [23] D. Balk, F. Pozzi, G. Yetman, U. Deichmann, and A. Nelson, "The distribution of people and the dimension of place: Methodologies to improve the global estimation of urban extents," in *Proc. Urban Remote Sens. Conf. Int. Soc. Photogramm. Remote Sens.*, Tempe, AZ, USA, Mar. 2005, pp. 849–857.
- [24] UT-Battelle, LLC, *Operator of Oak Ridge National Laboratory*, 2009, 2008 LandScan population dataset.
- [25] J. E. Dobson, E. A. Bright, P. R. Coleman, R. C. Durfee, and B. A. Worley, "LandScan: A global population database for estimating populations at risk," *Photogramm. Eng. Remote Sens.*, vol. 66, no. 7, pp. 849–857, Jul. 2000.
- [26] World Bank, *World Development Indicators*, 2013 (Last accessed June 9th, 2014). [Online]. Available: <http://data.worldbank.org/indicator>
- [27] C. N. H. Doll, *CIESIN Thematic Guide to Night-time Light Remote Sensing and its Applications*, 2008 (Last accessed June 9th, 2014). [Online]. Available: <http://sedac.ciesin.columbia.edu/tg/>
- [28] E. L. Glaeser, J. Gyourko, and R. E. Saks, "Urban growth and housing supply," *J. Econ. Geography*, vol. 6, no. 1, pp. 71–89, 2005.

- [29] I. G. Ellen and K. O'Regan, "Crime and urban flight revisited: The effect of the 1990s drop in crime on cities," *J. Urban Econ.*, vol. 68, no. 3, pp. 247–259, 2010.
- [30] S. S. Rosenthal, "Old homes, externalities, and poor neighborhoods. A model of urban decline and renewal," *Urban Econ.*, vol. 63, no. 3, pp. 816–840, May 2008.
- [31] P. Sutton, C. Roberts, C. Elvidge, and H. Meij, "A comparison of night-time satellite imagery and population density for the continental United States," *Photogramm. Eng. Remote Sens.*, vol. 63, pp. 1303–1313, 1997.
- [32] P. C. Sutton, D. Roberts, C. D. Elvidge, and K. Baugh, "Census from Heaven: An estimate of the global human population using night-time satellite imagery," *Int. J. Remote Sens.*, vol. 22, no. 16, pp. 3061–3076, 2001.
- [33] P. C. Sutton, C. Elvidge, and T. Obremski, "Building and evaluating models to estimate ambient population density," *Photogramm. Eng. Remote Sens.*, vol. 69, no. 5, pp. 545–553, 2003.
- [34] C. P. Lo, "Urban indicators of China from radiance-calibrated digital DMSP-OLS nighttime images," *Ann. Assoc. Am. Geographers*, vol. 92, no. 2, pp. 225–240, Jun. 2002.
- [35] C. N. H. Doll, J. P. Muller, and C. D. Elvidge, "Night-time imagery as a tool for global mapping of socio-economic parameters and greenhouse gas emission," *Ambio*, vol. 29, no. 3, pp. 157–162, May 2000.
- [36] P. C. Sutton, A. R. Goetz, S. Fildes, C. Forster, and T. Ghosh, "Darkness on the edge of town: Mapping urban and peri-urban Australia using nighttime satellite imagery," *Prof. Geographer*, vol. 62, no. 1, pp. 119–133, 2010.
- [37] M. L. Imhoff, W. T. Lawrence, D. C. Stutzer, and C. D. Elvidge, "A technique for using composite DMSP/OLS 'city lights' satellite data to accurately map urban areas," *Remote Sens. Environ.*, vol. 61, no. 3, pp. 361–370, Sep. 1997.
- [38] N. Zhao and E. L. Samson, "Estimation of virtual water contained in international trade products using nighttime imagery," *Int. J. Appl. Earth Observ. Geoinf.*, vol. 18, pp. 243–250, Aug. 2012.
- [39] T. Ghosh *et al.*, "Shedding light on the global distribution of economic activity," *Open Geography J.*, vol. 3, pp. 147–160, 2010.
- [40] C. N. H. Doll, J. P. Muller, and J. G. Morley, "Mapping regional economic activity from night-time light satellite imagery," *Ecol. Econ.*, vol. 57, no. 1, pp. 75–92, Apr. 2006.

Authors' photographs and biographies not available at the time of publication.